

2014

## HfC(310) High Brightness Sources for Advanced Imaging Applications

William A. Mackie


Josh M. Lovell

Todd W. Curtis

George Fox University, [tcurtis@georgefox.edu](mailto:tcurtis@georgefox.edu)

Gerald G. Megara

Follow this and additional works at: [https://digitalcommons.georgefox.edu/mece\\_fac](https://digitalcommons.georgefox.edu/mece_fac)

 Part of the [Atomic, Molecular and Optical Physics Commons](#), [Engineering Commons](#), and the [Engineering Physics Commons](#)

---

### Recommended Citation

Mackie, William A.; Lovell, Josh M.; Curtis, Todd W.; and Megara, Gerald G., "HfC(310) High Brightness Sources for Advanced Imaging Applications" (2014). *Faculty Publications - Biomedical, Mechanical, and Civil Engineering*. 42.

[https://digitalcommons.georgefox.edu/mece\\_fac/42](https://digitalcommons.georgefox.edu/mece_fac/42)

This Article is brought to you for free and open access by the Department of Biomedical, Mechanical, and Civil Engineering at Digital Commons @ George Fox University. It has been accepted for inclusion in Faculty Publications - Biomedical, Mechanical, and Civil Engineering by an authorized administrator of Digital Commons @ George Fox University. For more information, please contact [arolfe@georgefox.edu](mailto:arolfe@georgefox.edu).

# HfC(310) high brightness sources for advanced imaging applications

William A. Mackie,<sup>a)</sup> Josh M. Lovell, Todd W. Curtis, and Gerald G. Magera  
*Applied Physics Technologies, Inc., 1600 NE Miller Street, McMinnville, Oregon 97128*

The authors report on electron emission from HfC(310) operating in extended Schottky emission mode. Data are gathered from test stands as well as through operation in a commercial scanning electron microscope. Emitter end-form geometry consisted of rounded, via electrochemical etching, and truncated, via ion milling. The authors demonstrate high angular intensity operation of  $>60$  mA/sr especially for the rounded end-form emitters. Advantages include robustness of the material, which is not reliant on material supply as is the case with standard ZrO/W(100) sources. Hence, operation is available over a much larger range of temperatures, fields, and potentially pressures. Operation in a commercial scanning electron microscope gave ten times higher beam currents for identical operational parameters over a standard Schottky source.

## I. INTRODUCTION

We are working to demonstrate a new electron source for several applications where high brightness is required. This source would operate in the Schottky or extended Schottky emission (ESE) regime. Currently, cold field emission (CFE) sources and ZrO/W(100) Schottky sources are used commercially. CFE cathodes generally require lower pressures for stable operation and are prone to flicker noise but are electron optically very bright. Conventional Schottky sources are stable and reasonably bright but have limitations due to the supply of ZrO, which limit operations to a range of temperature (T), field (F), and pressure (P), hence limit angular intensity ( $I'$ ) and brightness or reduced brightness ( $B_r$ ).

Our new approach is to use transition metal carbides (TMCs). In general, these sources have high emission current capability, can be tolerant of moderate vacuum, are resistant to ion sputtering, and are capable of stable operation over a large temperature range.<sup>1,2</sup> HfC(310) specifically provides a relatively low work function ( $\sim 3.4$  eV), as a TMCs has a low evaporation rate,<sup>3</sup> a high melting point ( $\sim 4200$  K), and very low surface mobility. In this study, we operate in the ESE regime with temperatures from 1800 to 2000 K and fields to  $\sim 2 \times 10^9$  V/m.

In commonly used ZrO/W(100) Schottky sources and W CFEs, it is known that surface tension at high T contributes to blunting and atom migration at high F causes build-up. HfC emitters have activation energy for surface migration much larger than for W, which translates into very stable end-forms once obtained. Typical Zr/O/W sources are processed to facet the (100) plane at the apex.<sup>4</sup> However, the physical properties of HfC require us to artificially facet or truncate etched CFE type emitters in cases where a truncated end-form is desired.

## II. EXPERIMENT

### A. Material end-forms

Oriented single crystal material is prepared in our facility utilizing a floating zone refining system. The oriented rods

are centerless ground generally to  $\sim 0.5$  mm diameters, and then sectioned to  $\sim 2$  mm lengths. These are electrochemically etched to produce rounded end-forms as shown in Fig. 1(a). Etching techniques have been perfected to produce desired end-form radii in the range of  $50 \text{ nm} < r < 750 \text{ nm}$  with cone half-angle  $10^\circ < \theta < 30^\circ$ .

For cases where truncated tips are required, we use a FIB-system process of material removal to give the end-form shown in Fig. 1(b). The truncation diameters are generally in the range of  $30 \text{ nm} < D < 600 \text{ nm}$ .

### B. Angular intensity and angular distribution

We have operated many emitters of each style, rounded and truncated end-forms, in test stand systems. The common geometry consisted of emitter, suppressor, extractor, and screen with Faraday cup. Here, emitter protrusion from the suppressor was  $\sim 0.25$  mm, and suppressor-extractor separation was  $\sim 1$  mm. Table I shows data for several emitters operating under specified conditions and a range of angular intensities. The solid angle subtended by the Faraday cup was generally  $60\text{--}100 \mu\text{sr}$ .

The largest angular intensity values were obtained with the rounded end-forms. This was expected since the axial emission is peaked for rounded end-form emitters similar to CFE cathodes.<sup>5</sup> Standard faceted Schottky sources by comparison have the typical flat on-axis emission.<sup>4</sup>

### C. Noise

Electron emission variations or noise have long been studied and understood.<sup>6</sup> Two types of fluctuations typical to the emission of electrons from an emitter surface are flicker and shot. The most impact comes from flicker noise, which is related to surface diffusion and adsorption/desorption of adsorbate atoms. Flicker noise is prevalent at low frequencies ( $< 5$  kHz) and generally drops off as  $1/f$ .

There are several methods to acquire emission fluctuation information and a few standard means to display these data. The simplest means is to use a Faraday cup to collect beam or probe current and analyze the fluctuations found therein. Generally, this works well for frequencies of interest with 1

<sup>a)</sup>Electronic mail: bmackie@a-p-tech.com

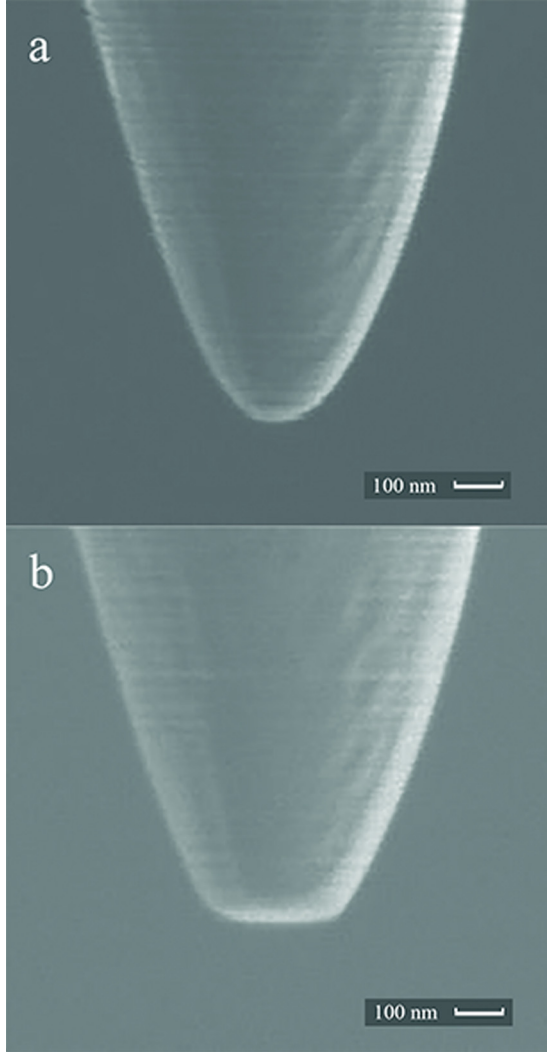


FIG. 1. (Color online) (a) Etched HfC(310) tip with  $\sim 100$  nm tip radius. (b) Micrograph of same tip after FIB removal of apex creating a  $\sim 220$  nm diameter flat.

$\text{Hz} < f < 1 \text{ kHz}$ . Practically,  $\sim 1 \text{ kHz}$  is a limit for this method due to capacitance found in association with the Faraday cup geometry. After the calculation of  $I'$  the mean noise was obtained by

$$\frac{|(I' - I'_{\text{ave}})|}{I'_{\text{ave}}}. \quad (2)$$

These data are shown in Table II and combines the authors previous work with values obtained in this study. For comparison, one point is show for a standard ZrO/W source; all values generated were at 500 Hz.

The noise comparisons shown in Table III are for three emitters; two with rounded end-form and one with a FIB truncated emitter. The operating temperatures were the same for each at 1900 K.

We can see that the noise is inversely proportional to the emitter radius for the rounded tips and is much lower for the truncated tip. These experimental data verify modeling and shows a possible benefit of the FIB truncated HfC(310)

TABLE I. Angular intensity for HfC(310) sources with round and truncated end-forms.

Emitter type	Radius (nm)	Temp. (K)	$V_{\text{ext.}}$ (V)	$I'$ (mA/sr)
HfC(310)—AF011	350 (trunc.)	1900	3.0	0.5
HfC(310)—AF104	150 (trunc.)	1900	3.2	1.2
HfC(310)—AF047	400 (trunc.)	1900	2.5	0.5
ZrC(310)—AF040	280 (round)	2000	4.2	61.1
HfC(310)—AF078	200 (round)	1800	3.8	12.0
HfC(310)—AF088	450 (round)	1800	4.9	30.0

emitters operated in Schottky emission mode. Reasoning is that for the truncated emitter the noise is less as the field shaping around the tip means that the emission area is slightly larger for a given extractor geometry. Hence, the number of emission sites is larger, and the average noise is lower.

#### D. Energy spread

Field emission theory shows extremely high potential current densities from cold field emitters. Thermionic emission (TE) and CFE are the two end points in a continuum of electron emission processes, in between lays the thermal-field (TF) emission regime and ESE. Stability generally favors TE where the most stable cathode would perhaps be a TE emitter operated in space-charge mode. The sense is reversed with brightness where CFEs comprise the brightest possible emitter.

Electronic energy spread ( $\Delta E$ ) depends upon the emission regime but is peaked in the central temperature or TF region.<sup>4,7</sup> The peak in  $\Delta E$  depends upon work function and current extraction levels. Figure 1.25 of Ref. 4 shows plots of  $\Delta E$  versus temperature for several modeled emitters with a range of work functions but at similar emitted current densities.  $\Delta E$  values are calculated as full-width half-maximum (FWHM) of the distribution curve, and in the room temperature, CFE operation all curves have  $\sim 250 \text{ meV}$  energy spread, peak in the central region, and drop at higher temperatures. Similar energy spreads of  $\sim 400\text{--}600 \text{ meV}$  for the  $3.0 \text{ eV}$  source operated at 1800 K and the  $3.5 \text{ eV}$  source operated at 2000 K mimicking ZrO/W and HfC Schottky sources, respectively.

TABLE II. Noise (at 500 Hz) of HfC cathode over temperatures, emitter radius was  $\sim 200$  nm, also shown is one point for a ZrO/W source ( $\sim 450$  nm facet diameter).

Temperature (K)	Mean noise % (previous study)	Mean noise % (this study)	Mean noise % ZrO/W
300	0.08		
660	0.20		
880	0.29		
1600		0.41	
1700		0.21	
1800		0.11	0.07
1900		0.04	
2000		0.02	

TABLE III. Mean noise (at 500 Hz) of HfC(310) tips at 1900 K with varying end-forms.

Tip #	Tip type	Mean noise %
AF078	Etched, rounded, $r \sim 200$ nm	0.0286
AF088	Etched, rounded, $r \sim 750$ nm	0.0208
AF011	FIB truncated	0.0063

We used a filter lens retarding energy analyzer<sup>8</sup> to obtain FWHM data for an HfC emitter at several temperatures up to 1250 K. These data agree with theory<sup>9</sup> (see Fig. 2) but due to issues with the analyzer we were precluded from obtaining meaningful data at higher temperatures.

### E. Commercial SEM modifications

In these tests, we used a Philips XL40 field emission gun (FEG) SEM. Several modifications were required as delineated here. Due to the brittle nature of crystalline HfC, we are unable to spot weld the shank to a conventional filament for heating. The authors have previously described the components of a Vogel type mount<sup>10</sup> but will summarize the needed configuration for using HfC(310) Schottky sources in commercial FEG module.

Figure 3 shows a completed mount with an HfC Schottky source having several changes to conventional Vogel mounted cathodes. First, a shunted mini Vogel mount (SMVM) is used where Re shunts change the heater characteristics to better mimic a filament type mount. Second, we use a smaller emitter crystal than has been common in the past. This reduces the surface area and the power radiated at temperature, hence reducing the heater power. Next, we use smaller than normal inner pyrolytic graphite blocks, which also serves to reduce heater power levels. Finally, shields are added to eliminate the chance of leakage current due to deposition on the ceramic base.

In a commercial Zr/O/W(100) Schottky source, the suppressor and nominally the extractor apertures have a  $\sim 375$   $\mu\text{m}$  diameter. The extractor-suppressor spacing is  $\sim 0.75$  mm, and the tip protrudes  $\sim 0.25$  mm above the suppressor. The W(100) wire in most commercial sources has a 0.005-in. diameter. Due to the larger crystal diameter for the

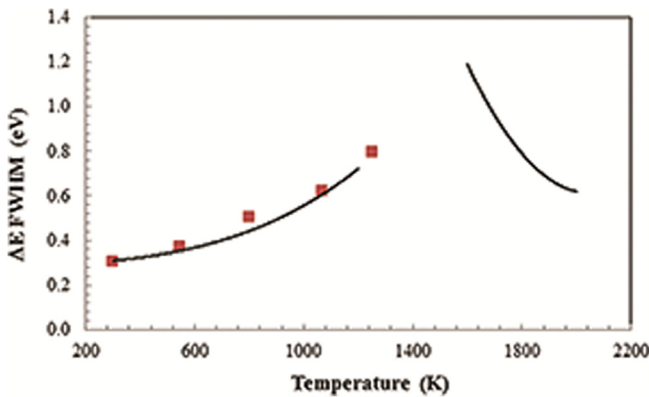


FIG. 2. (Color online) Theoretical curve and measured values of  $\Delta E$  (FWHM) for HfC source. The model assumes work functions of 3.5 eV, a tip radius of 200 nm, and a field of 2.4 V/nm.

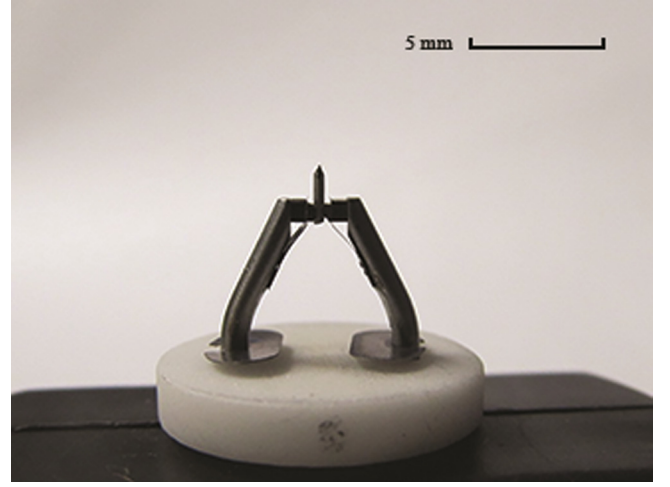


FIG. 3. (Color online) Completed Vogel-type mount for HfC(310) Schottky source which operates at  $\sim 3.4$  W for 1800 K.

carbide emitter (nominally  $3\times$ ), the suppressor aperture needed to be enlarged. These modifications were accomplished by making a new suppressor housing having the same outside dimensions as the conventional suppressor used on the XL-40, but modified internally to accommodate the Vogel style mount, ceramic base, and larger aperture.

We also found that the suppressor/extractor sections failed due to the epoxy type glue used to bond the metal parts to the  $\text{Al}_2\text{O}_3$  ceramic section. With the somewhat higher heater power (up to  $3\times$ ) used in the HfC source, this glue outgasses at an extreme rate, which caused very high local pressures, reduced emission from the tip, and eventual failure of the glued joint. The solution was to use vacuum brazing for the parts in the FEG module.

## III. RESULTS AND DISCUSSION

### A. Images

Many SEM micrographs were taken using the HfC source and qualitative comparisons made to micrographs previously taken using the Zr/O/W source. Comparison images were viewed and found similar in resolution but the limiting factor in most cases was system vibration reflective of the SEM's physical location in our facility. The images shown in Figs. 4(a) and 4(b) were taken with similar SEM settings and are of evaporated gold particles taken with a ZrO/W source and an HfC source respectively, at 100,000 $\times$  magnification. Specific operating conditions were 1200 mm aperture, spot size 3, 10 kV beams, and both emitters at 1800 K. The ZrO/W had a facet radius of  $\sim 230$  nm, and the HfC had a rounded end-form with a radius of  $\sim 150$  nm.

### B. Beam currents

Due to emitter end-form geometry differences, we were able to obtain much higher beam currents with HfC as compared to Zr/O/W sources for exactly the same SEM operating conditions. Shown in Fig. 5 are comparisons using 1200  $\mu\text{m}$  apertures. Similar results were found using a 60  $\mu\text{m}$  aperture. As compared, the rounded (radius =  $\sim 150$  nm)



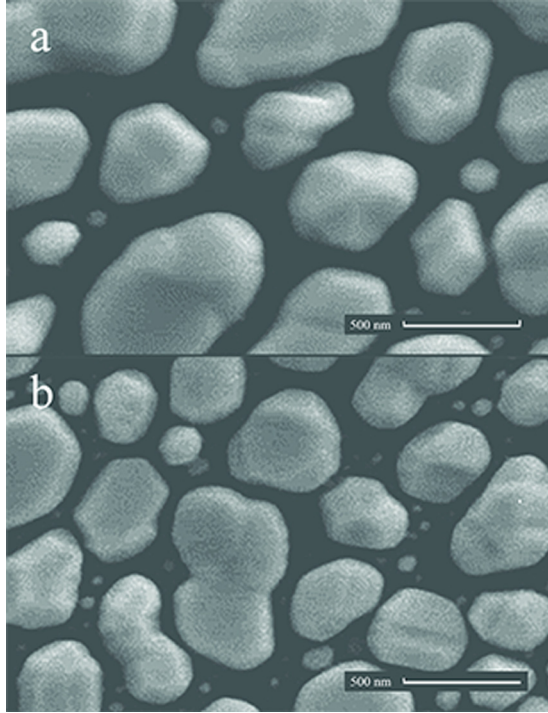


FIG. 4. (Color online) SEM images (a) using a ZrO/W source and (b) using an HfC source. Both operating at 1800 K with identical SEM settings; beam voltage 10 kV, 60  $\mu\text{m}$  aperture, and SEM spot size 3. The extraction voltages and total emission currents were 4600 V and 158  $\mu\text{A}$  for the ZrO/W and 3950 V and 108  $\mu\text{A}$  for the HfC.

HfC(310) source has  $\sim 10\times$  higher beam currents. The horizontal axis is actually the “column” current in  $\mu\text{A}$  as measured in the drift tube of the SEM prior to the beam limiting aperture. The drift tube current is proportional to the average angular intensity setting of the emitter since we collect a total current for a given solid angle; here, a current of  $\sim 8\ \mu\text{A}$  translates to an average  $I'$  of  $\sim 0.4\ \text{mA/sr}$ . These values were set for each emitter and the beam current hitting the sample measured. The sample in these cases was a Faraday cup on the SEM stage. We are therefore comparing like setting with each source and see the higher axial current delivered in the beam for the HfC source. This could translate into faster imaging due to the increase in signal strength.

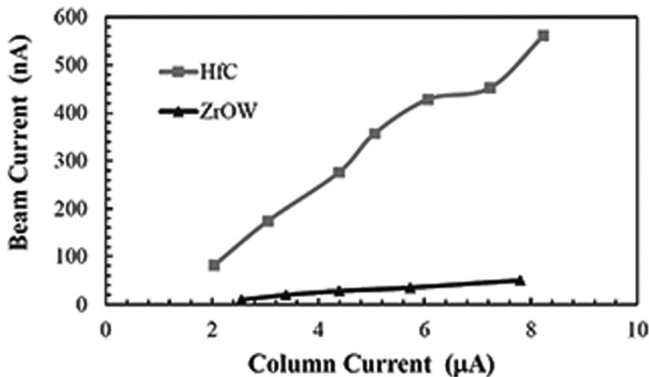


FIG. 5. Measured beam currents compared using the 1200  $\mu\text{m}$  aperture and identical SEM settings. The extraction voltage range differed slightly; the ranges shown were 3.5–4.5 kV and 4.0–5.0 kV for the ZrO/W and HfC sources, respectively.

TABLE IV. Spot parameter measurements compared.

Emitter	Truncation (D)/radius (R)	Spot size
ZrO/W(100)	D = $\sim 300\ \text{nm}$	26.4 nm
HfC(310)—tip #137	D = $\sim 200\ \text{nm}$	19.0 nm
HfC(310)—tip #130	D = $\sim 125\ \text{nm}$	13.2 nm
HfC(310)—tip #132	R = $\sim 150\ \text{nm}$	9.9 nm

### C. P-Parameter

We also obtained a “performance parameter” or effective beam size generated during SEM operation. This method is summarized in an American Society for Testing and Materials publication.<sup>11</sup> Since single crystal HfC cleaves nicely along the (100) crystallographic plane it was used as the sharp edge needed. The SEM was operated at 100,000 $\times$  magnification, and a line scan was generated over the sharp edge. The minimum and maximum values are noted and the 20% and 80% values are calculated. The width between these 20%/80% points were found using the image software available on the SEM.

This method generated physical beam size measurements using several HfC(310) Schottky sources and a commercial ZrO/W(100) source. Identical SEM spot size setting was used for each measurement. Table IV shows a summary of measured spot sizes for the ZrO/W emitter and three HfC emitters, two truncated and one rounded. This P-parameter seems to scale with facet or truncation size, but it is interesting to note that the rounded emitter gave the smallest value.

## IV. SUMMARY

Initially, we had identified several risks associated with these HfC emitters. These included energy spread, noise, the Vogel mount, and the stability of the HfC material. We now comment on these based on the data collected thus far.

### A. Energy spread

Modeling demonstrates that  $\Delta E$  peaks in the TF emission regime but falls again in the ESE mode. The entire curve shifts with higher work functions; HfC(310) is  $\sim 0.5\ \text{eV}$  larger than ZrO/W(100). However, operating the emitter at higher temperatures can partially offset the higher work function. This has been shown through modeling, and we have also taken experimental energy spread data which support the modeling at least at the lower temperatures. Further work is required to obtain  $\Delta E$  values in the 1800–2000 K range.

### B. Noise

We have shown that flicker noise levels are similar as for conventional Schottky emitters. There is a proviso that the end-form of the emitter does play a role in the emission area, which impacts stability where the FIB faceted end-form is more stable than the rounded CFE type end-form.

### C. Vogel mount

These mounts have proven to be very stable mechanically and have shown satisfactory operation at high temperatures

for long periods of time. We are now able to adjust the mounting slightly and to some degree tune-in the power consumption required for a given operating temperature.

#### D. Material stability

This material has proven very robust thermally, chemically, and in regards to shape change through surface diffusion. The material risk factor remains very low.

#### V. CONCLUSIONS

With this project, we have documented the utility of the HfC(310) cathode operating in ESE mode. Benefits can be derived from the refractory nature and not needing a supply function. These factors expand the temperature and field ranges of operation. It can be shown that these sources are optically very bright compared to the standard Zr/O/W(100) source, especially for the rounded end-form due to the peaked angular distribution of emission on-axis. The imaging effort shows the promise of the material though more work could be done to optimize the SEM optical system to make use of the brighter source.

We are able to form a range of truncated emitter end-forms through our etch process coupled with FIB micromachining. We have shown that angular intensity values for HfC(310) Schottky emitters can be significantly broader than for conventional Zr/O/W(100) Schottky sources, respectively,  $<0.1 \text{ mA/sr} < I' < 60 \text{ mA/sr}$  compared with the fairly strict range  $0.2 \text{ mA/sr} < I' < 1.0 \text{ mA/sr}$ .<sup>4</sup> We have seen

stable emission to  $5 \times 10^{-8}$  Torr levels and are in the process of determining if that range can be expanded. Finally, we have demonstrated that these cathodes can be operated in a commercial SEM with relatively little retrofitting.

#### ACKNOWLEDGMENTS

The authors would like to thank Joe Hancock for electronics and vacuum system support. Financial support was provided in part by Air Force Research Laboratory (AFRL).

<sup>1</sup>W. A. Mackie, R. L. Hartman, and P. R. Davis, *Appl. Surf. Sci.* **67**, 29 (1993).

<sup>2</sup>W. A. Mackie, J. L. Morrissey, C. H. Hinrichs, and P. R. Davis, *J. Vac. Sci. Technol. A* **10**, 2852 (1992).

<sup>3</sup>W. A. Mackie and P. R. Davis, *IEEE Trans. Electron. Devices* **36**, 220 (1989).

<sup>4</sup>L. W. Swanson and G. A. Schwind, in *Handbook of Charged Particle Optics*, 2nd ed., edited by J. Orloff (CRC, New York, 2008).

<sup>5</sup>R. Gomer, *Field Emission and Field Ionization* (Harvard Univ. Press, Cambridge, MA, 1961).

<sup>6</sup>L. W. Swanson and A. E. Bell, *Adv. Electron. Electron Phys.* **32**, 193 (1973).

<sup>7</sup>H. Adachi, Y. Shibuya, T. Hariu, and Y. Shibata, *J. Phys. D: Appl. Phys.* **10**, L113 (1977).

<sup>8</sup>J. A. Simpson, *Rev. Sci. Instrum.* **32**, 1283 (1961).

<sup>9</sup>Michael R. Scheinfein, *LLG Micromagnetics Simulator*, Beaverton, OR 97005.

<sup>10</sup>W. A. Mackie and G. G. Magera, *J. Vac. Sci. Technol. B* **29**, 06F601 (2011).

<sup>11</sup>ASTM International, "Standard practice for scanning electron microscope beam size characterization," Designation: E 986-04. See: [www.astm.org](http://www.astm.org), 2004.